

# Visual Analytics for Electromagnetic Situation Awareness in Radio Monitoring and Management

Ying Zhao, Xiaobo Luo, Xiaoru Lin, Hairong Wang, Xiaoyan Kui, Fangfang Zhou, Jinsong Wang, Yi Chen, and Wei Chen

**Abstract**—Traditional radio monitoring and management largely depend on radio spectrum data analysis, which requires considerable domain experience and heavy cognition effort and frequently results in incorrect signal judgment and incomprehensive situation awareness. Faced with increasingly complicated electromagnetic environments, radio supervisors urgently need additional data sources and advanced analytical technologies to enhance their situation awareness ability. This paper introduces a visual analytics approach for electromagnetic situation awareness. Guided by a detailed scenario and requirement analysis, we first propose a signal clustering method to process radio signal data and a situation assessment model to obtain qualitative and quantitative descriptions of the electromagnetic situations. We then design a two-module interface with a set of visualization views and interactions to help radio supervisors perceive and understand the electromagnetic situations by a joint analysis of radio signal data and radio spectrum data. Evaluations on real-world data sets and an interview with actual users demonstrate the effectiveness of our prototype system. Finally, we discuss the limitations of the proposed approach and provide future work directions.

**Index Terms**—Radio monitoring and management, radio signal data, radio spectrum data, situation awareness, visual analytics

## 1 INTRODUCTION

Radio communication is a technology that modulates electrical signals (e.g., sounds and images) onto electromagnetic waves to transmit information through space. The electromagnetic spectrum is an indispensable but finite natural resource for carrying electromagnetic waves. Any electromagnetic wave must occupy a small contiguous section of the electromagnetic spectrum for information transmission. With the explosive growth of various radio devices (e.g., cellphones, Wi-Fi, and radars), the demand for the spectrum resource has rapidly increased. This increment has led to increasingly complex electromagnetic environments.

Radio supervisors in radio administration bureaus are in charge of radio monitoring and management (RMM) within their jurisdictions to achieve the orderly use of the spectrum resource. Their daily work can be described as a top-down process of situation awareness on electromagnetic environments. First, they regularly sense the overall situation of frequency occupancy in a monitoring band. Second, they recognize important or high-risk sub-bands and identify existing radio signals. Finally, they detect, explicate, and prevent communication anomalies, such as the unsteadiness of authorized signals and the illegal spectrum occupations of unauthorized signals.

For a long time, the daily work of radio supervisors has largely depended on the analysis of radio spectrum data (SpeData). SpeData are collected by sensing equipment and converted from analog-to-digital (AD) sampling sequence data (Figure 1(a–c)). As semi-structured data, SpeData can reflect the spectrum occupancy situation but cannot directly reveal existing radio signals and their characteristics. Hence, radio supervisors need to view traditional spectrum diagrams [4, 23] (e.g., amplitude-frequency

and time-frequency diagrams, as shown in Figure 2(a–b)) all the time. Consequently, RMM requires considerable domain experience. Radio supervisors commonly suffer from heavy cognition load. Incorrect signal judgment and incomprehensive situation awareness frequently occur in their daily work.

Introducing additional data sources into RMM is an inevitable trend [24]. Radio signal data (SigData) are fully structured data extracted from SpeData (occasionally combined with AD sampling sequence data) through a series of complicated signal processing procedures (Figure 1(d)). As a new RMM data source, SigData have preliminarily identified existing radio signals and their characteristics, which will help reduce the requirements of domain experience and the cognition burden of radio supervisors. However, several challenges remain in practice. First, a non-instantaneous radio signal is recorded multiple times in SigData because of the ongoing communication monitoring. Second, traditional spectrum diagrams cannot properly depict the time-frequency distribution and multidimensional time-varying patterns of characterized radio signals in SigData (Figure 2(c–d)). Lastly, radio supervisors require advanced tools to help them assess, perceive, and understand complex electromagnetic situations through the joint use of SigData and SpeData.

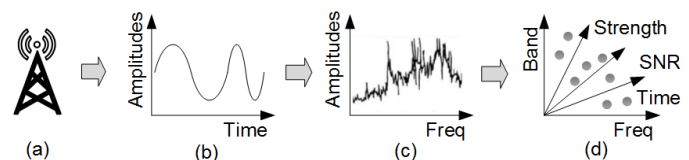


Figure 1. Acquisition of SpeData and SigData: (a) radio sensing equipment, (b) AD sampling sequence data, (c) SpeData converted from AD sampling sequence data through fast Fourier transform, and (d) SigData extracted from SpeData and AD sampling sequence data.

- Ying Zhao, Xiaobo Luo, Xiaoru Lin, Hairong Wang, Xiaoyan Kui, and Fangfang Zhou are with School of Computer Science and Engineering, Central South University, Changsha, Hunan, China. E-mails: {zhaoying, luoxiaobo, 0904130203, hairongwang, kuixu, zff}@csu.edu.cn;
- Jinsong Wang is with Southwest Electric & Telecom Engineering Institute, Shanghai, China. E-mail: jinsong.wang@126.com;
- Yi Chen is with Beijing Key Laboratory of Big Data Technology for Food Safety, Beijing Technology and Business University, Beijing, China. E-mail: chenyi@th.btbu.edu.cn;
- Wei Chen is with State Key Lab of CAD & CG, Zhejiang University, Hangzhou, Zhejiang, China. E-mail: chenwei@cad.zju.edu.cn.
- Xiaoyan Kui and Fangfang Zhou are corresponding authors.

Manuscript received xx xxx. 201x; accepted xx xxx. 201x. Date of Publication xx xxx. 201x; date of current version xx xxx. 201x. For information on obtaining reprints of this article, please send e-mail to: reprints@ieee.org. Digital Object Identifier: xx.xxx/TVCG.201x.xxxxxx

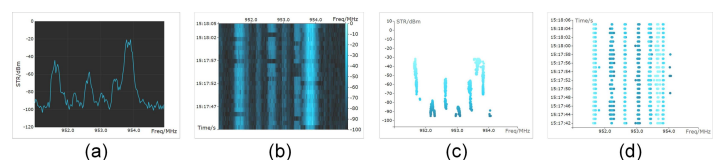


Figure 2. Traditional spectrum diagrams used to visualize SpeData and SigData: (a) a SpeData frame in a spectrum amplitude-frequency diagram, (b) a group of sequential spectrum frames in a spectrum time-frequency diagram, (c) SigData in a spectrum amplitude-frequency diagram, and (d) SigData in a spectrum time-frequency diagram.

In this study, we propose a visual analytics approach to help radio supervisors achieve an efficient and comprehensive electromagnetic situation awareness. A new signal clustering method is proposed to address the issue of duplicate signal records in SigData. By adopting the divide-and-conquer concept, the proposed method applies a grid division to distinguish dense and sparse areas of signal records in the data space composed of frequency and bandwidth. Then, an improved density clustering algorithm is utilized to apply different clustering treatments for the two area types. Moreover, we fully consider the role of detection time, strength, and signal-to-noise ratio (SNR) to further improve the accuracy of SigData clustering.

A novel signal time-frequency (STF) diagram is designed to help radio supervisors interactively analyze SigData. The STF diagram is equipped with two visualization modes. The first is the river mode, which adopts a river metaphor to encode a signal's four basic characteristics along a time axis. Thus, radio supervisors can easily perceive the time-frequency distribution and multidimensional time-varying patterns of signals during real-time monitoring. The second is the scatter mode, which provides three scatterplot encoding styles and rich interactions to enable radio supervisors to perform multi-perspective and interactive SigData exploration when communication anomalies occur.

We design and implement a visual analysis prototype system to help radio supervisors assess, perceive, and understand electromagnetic situations. The system consists of a qualitative and quantitative situation assessment model and an interactive interface. For the situation assessment model, we consider various influencing factors in the design of a situation assessment index system. Then, we utilize diverse computational analysis methods to derive qualitative and quantitative situation descriptions. For the interface, a two-module design that includes a monitoring module and an exploring module is applied to support interactive situation perception and understanding. The monitoring module, which contains a situation visualization view and a river-mode STF diagram, aims to help radio supervisors quickly perceive the overall electromagnetic situation and signal distribution of the monitored band. The exploring module, which contains a scatter-mode STF diagram and two spectrum diagrams, is designed to promote the joint analysis of SigData and SpeData. This joint analysis can help radio supervisors understand high-risk situations and explore the root causes of communication anomalies. To evaluate our approach, we conducted a signal clustering experiment and a case study using real-world data sets. We also interviewed two target users.

The main contributions of this work are as follows:

- A signal clustering method that integrates multiple clustering strategies and considers multiple signal characteristics to process SigData;
- An STF diagram that visualizes the results of signal clustering and supports interactive SigData explorations;
- A visual analysis prototype system that helps users assess, perceive and understand complex electromagnetic situations.

## 2 RELATED WORK

### 2.1 Visualization for RMM

RMM has undergone three technological revolution stages, namely, informationization, networking, and intellectualization. The rapid development of information technology at the end of the 20th century led to the emergence of various software and hardware systems for RMM. The networking stage of about 10 years interconnected a large number of radio sensing equipment to support gridding and seamless RMM. In the current intellectualization stage, cognitive radio technologies [6, 54] drive new levels of high-throughput and low-interference radio spectrum multiplexing, and advanced data analysis technologies [9, 50] gain insights from various data resources to promote management innovation. Our work belongs to advanced data analysis for RMM innovation.

With the evolution of the visualization community, visualizations for RMM have experienced three development phases, namely, scientific visualization [51], information visualization [37, 57, 61, 73, 74], and visual analysis [11, 20, 66, 67, 76]. Scientific visualization in this domain focuses on electromagnetic field simulations, which involve 3D graphical representations of simulation data generated by computational models of electromagnetic radiation phenomena of radio signal sources. Electromagnetic field simulations are mainly applied in military and aerospace fields.

A few studies have been conducted on radio astronomy and commercial software. For example, Hassan et al. [39] visualized the electromagnetic radiation phenomena of the entire Milky Way by using a distributed volume rendering. Vijgen [1] developed an iPad application for displaying radio signal locations such as Wi-Fi and cell phone towers.

Information visualization in this domain generally refers to spectrum visualizations, which visualize SpeData to help people observe the distributions of radio signals in terms of frequency, signal strength and time. Spectrum amplitude-frequency and time-frequency diagrams [4, 23] are well-known visualizations that have been widely used in commercial software and hardware systems, such as Rohde & Schwarz and TEK product families [2, 3]. Meanwhile, a few improved visualizations have been reported. For example, Kincaid [41] integrated a Focus+Context interaction into a classic amplitude-frequency diagram. Chen et al. [17] and Sharakhov et al. [58] proposed 3D time-frequency diagrams.

Radio administration bureaus currently face with various data resources and increasingly complex analytical tasks. Thus, traditional electromagnetic field simulations and spectrum visualizations need to be extended to visual analysis with high data cooperation and strong human-computer interactivity [12, 25, 31]. Only a few pioneering researchers have worked on this issue. Crnovrsanin et al. [24] proposed the first visual analytics approach for RMM. The authors integrated wavelet and principal component analyses to process SigData, and provided a multi-view interactive interface to help radio managers recognize and locate special signals and signal repeaters in a monitored area. Cantu et al. [15] constructed the first 3D immersive visual analysis environment for multidimensional radar signal data analysis.

Our work differs from the aforementioned visual analysis studies in two aspects. First, two types of data are used simultaneously in our work to accomplish analytical tasks that require close data cooperation. Second, our work focuses on the situation awareness of electromagnetic environments, which is a completely new scenario of applying visual analysis in RMM.

### 2.2 Visualization for Situation Awareness

The concept of situation awareness was proposed by Endsley [32]. Early studies mainly focused on the design of advanced situation assessment models or algorithms. In recent years, human-centered visualization and visual analysis methods [19, 28, 53] have been introduced into the entire process of situation awareness, including situation perception, understanding, and even prediction. Many important achievements have been obtained in a wide range of application domains [7, 16, 36, 62]. For example, VisFlowConnect [72], NVsionIP [44], and VisAlert [48] are famous visualization approaches for cyber security situation awareness. Ebert et al. [42] proposed a large-scale visual analysis system to facilitate the situation awareness of infrastructure security when a city or country encounters natural disasters. Zhou et al. [75] designed a visual analysis system to help users perceive and understand the current operating situation of a complex manufacturing facility. Ross et al. [49, 55] developed a set of interactive situation awareness tools for the community crime prediction. This study can be regarded as the first attempt to introduce visual analysis technologies into electromagnetic situation awareness.

### 2.3 Visualization for Time Series Analysis

Extensive research has been conducted on the visualization and analysis of time series data [5]. The methods proposed by these studies can be categorized into theoretical, technological, and application approaches. Theoretical approaches aim to explore the principles and rules of visual designs and visual perceptions of time-varying patterns [13, 35]. Technological approaches propose new time series visualizations [40, 43, 52] or improve existing visualizations [8, 30, 47]. The application approaches focus on addressing the tasks and challenges of time series data analysis in specific scenarios [21, 45, 68], such as medical diagnosis [22, 69], topic evolution in social media [26, 27], and behavior analysis in a wide range of application domains [18, 59, 63, 70]. Our work is an application approach. In the application domain of RMM, several studies have been conducted to improve traditional spectrum diagrams [17, 58], but a few studies have performed the time-varying pattern analysis of electromagnetic situations and signal characteristics. We consulted many time series visualization studies to guide our visualization design. We obtained considerable inspirations from pixel [38, 60, 65], flow-style [47, 61, 76], and river-style

visualizations [14, 40, 43].

### 3 DATA, SCENARIO, AND REQUIREMENT

#### 3.1 Data Abstraction

SpeData formatted in frequency frames are generally used in RMM. As shown in Figure 1(a–c), a frequency frame has a group of information elements, including sensing time, frequency band, number of frequency points, and frequency spectrum array. For example, a certain frame has a frequency band ranging from 900 MHz to 950 MHz with 1,024 frequency sampling points equally distributed in the band. Its frequency spectrum array records the signal amplitudes of all the frequency points at a certain moment. Relatively high amplitudes indicate that the corresponding frequency points may be occupied by radio signals. As a result, SpeData effectively reflect the distribution of occupied frequencies in a monitoring frequency band but cannot directly indicate the number of actual radio signals existing in the band.

SigData are extracted from SpeData, as shown in Figure 1(d). SigData are fully structured in the form of multidimensional data records with time information. A SigData record, also known as a signal feature vector (SFV), presents the basic signal characteristics of a detected radio signal, mainly including detecting time, center frequency, bandwidth, strength, and SNR. For instance, a certain SFV indicates that a radio signal with a center frequency of 950 MHz, a bandwidth of 2,101 MHz, a strength of  $-69$  dBm, and a SNR of 50 dB was detected at 9:30:05 am. Accordingly, SigData characterize the radio signals that may actually exist.

#### 3.2 Scenario and Challenges

Our target users are radio supervisors in radio administration bureaus who are responsible for monitoring the electromagnetic environments of special areas (e.g., airports, harbors, and power stations) and maintaining the normal communication of several important signals (e.g., air traffic control tower communication or mobile communication). Traditionally, supervisors conduct their daily work largely through the SpeData analysis assisted by spectrum amplitude-frequency and time-frequency diagrams (Figure 2(a–b)). The recent introduction of SigData is expected to reduce the time and effort exerted by supervisors because SigData provide characterized information on radio signals. However, supervisors still encounter the following challenges in practice.

**C1: SigData clustering.** Signal clustering is a procedure in radio signal processing that separates actual non-instantaneous signals from radiation sources and sensing data sets on the basis of the signals' core characteristics (i.e., center frequency and bandwidth). Any non-instantaneous signal is normally recorded multiple times in SigData because of continuous monitoring. Thus, clustering SFVs is a necessary data preprocessing task. However, this task is difficult for many reasons. First, possible environmental noises and signal interferences cause the SFVs' values in the same signal to fluctuate within a certain range. Second, the number of actual signals in a monitoring band is generally unpredictable, and their distributions in frequency and bandwidth may be uneven. Third, several communication systems, such as adaptive frequency and hopping spectrum technologies, make it difficult to clustering is essential for real-time monitoring.

**C2: Presenting the patterns of radio signals in frequency and time.** Supervisors are accustomed to utilizing spectrum amplitude-frequency and time-frequency diagrams to obtain the overall situation of spectrum occupancy from semi-structured and nearly continuous SpeData. However, massive scattered data points are observed when fully structured SigData are presented by these diagrams, as shown in Figure 2(c–d). Thus, supervisors cannot perceive the spectrum occupancy situation nor determine the time-varying patterns of signal characteristics.

**C3: Achieving comprehensive situation awareness.** Electromagnetic environments are complicated and change constantly. Situation assessment normally requires the full consideration of various factors, and situation understanding entails a thorough analysis of sufficient contextual information. The use of SigData facilitates the introduction of advanced analytics into supervisors' daily work. New tools are required to help supervisors achieve an efficient and comprehensive situation awareness.

### 3.3 Requirement Analysis

We conducted a series of in-depth and meticulous research procedures, including face-to-face interviews, discussions, and preliminary data analysis, on our target users to understand the users' requirements. We formulated two requirements (R1–R2) for automatic data analysis and four requirements (R3–R6) for interactive data analysis to guide our study.

**R1: Cluster SigData accurately and efficiently.** Signal clustering is the first step of using SigData in RMM. An appropriate method is required to quickly obtain reasonable clustering results from SigData.

**R2: Evaluate the electromagnetic situations quantitatively and qualitatively.** Numerous factors should be considered when creating measurable and comprehensive situation descriptions. The descriptions can guide the subsequent data analysis.

**R3: Support intuitive situation perception.** The calculation results of the situation assessment model should be presented in an intuitive manner. Accordingly, users can easily perceive the current situation, its recent change trend, and high-risk frequency sub-bands.

**R4: Visualize the results of signal clustering.** Users require a new diagram to visualize the results of signal clustering so that they can identify the distribution and time-varying patterns of the signals currently existing in the monitoring band.

**R5: Facilitate deep situation understanding.** An interactive data analysis tool is required to involve users in the analysis of contextual information for situation understanding because their domain experience is essential in explaining the causes of anomalies.

**R6: Use familiar visual metaphors and lightweight interactions.** Most target users lack sufficient experience in using visual analysis systems. The visual design should be easy to read, and the interactive operations should be easy to use.

## 4 SYSTEM OVERVIEW

We design a visual analysis prototype system to help radio supervisors assess, perceive, and understand electromagnetic situations. The system workflow is shown in Figure 3. After the preparation of SigData and SpeData, the system primarily includes two phases. In the computational analysis phase, we initially perform a signal clustering process on SigData (R1). Then, we conduct a situation assessment on the basis of the clustering results (R2). In the interactive analysis phase, we provide radio supervisors with an interactive interface. The interface uses a monitoring module to present the results of situation assessment and signal clustering for situation perception (R3, R4). It also contains an exploring module to provide a joint analysis of SigData and SpeData for situation understanding (R5). On the basis of the observation and exploration in the interactive analysis phase, users can reset the parameters of the computational methods to obtain new signal clustering and situation assessment results. They can even directly adjust the signal clustering results on the interactive interface (R6).

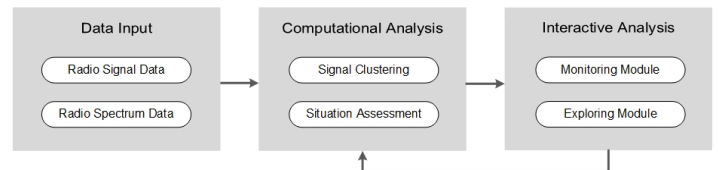


Figure 3. System workflow.

## 5 COMPUTATIONAL ANALYSIS

### 5.1 Signal Clustering

Signal clustering identifies actual radio signals in SigData in accordance with the basic rule that the SFVs of the same signal should have a similar center frequency and bandwidth. Each cluster represents an actual radio signal. However, traditional clustering methods (e.g., k-means and DB-SCAN) experience difficulties in achieving accurate and efficient signal clustering as mentioned in C1. We propose a new method for clustering signals in SigData. This section elaborates the five major steps of the proposed method.

#### 5.1.1 Grid Division

Radio communication often presents an uneven signal distribution. A number of radio signals may be crowded in a narrow frequency band

or have a similar bandwidth. In this work, we use a grid division to distinguish the areas with dense and sparse SFV distributions in the data space composed of frequency and bandwidth. In this manner, different clustering strategies can be used in the two types of areas to reduce the impact of the uneven signal distribution on the accuracy and efficiency of signal clustering. Specifically, we initially divide each dimension of the frequency-bandwidth data space into  $m$  equal-sized grids. Then, we calculate the number of SFVs in each grid. Finally, we distinguish dense and sparse grids on the basis of a density threshold  $MinPts$ . Referring to [71], we set the grid number  $m$  with  $\sqrt{N}$ . Referring to [29], we measure the density threshold  $MinPts$  with the average density of non-empty grids. The two settings are expressed as

$$m = \text{int}(\sqrt{N}), \quad MinPts = \left( \sum_{i=1}^z \frac{density_i}{z} \right), \quad (1)$$

where  $N$  represents the total number of SFVs,  $z$  represents the number of non-empty grids, and  $density_i$  denotes the density of a non-empty grid.

### 5.1.2 Dense Area Processing

Empirically, most SFVs in dense grids are constant signals because of continuous and long-term communication. As identity characteristics, the center frequency and bandwidth of a constant signal are supposed to be constant during communication, although small fluctuations in the two characteristics may occasionally occur. Therefore, SFVs with a compact Gaussian convex distribution and a clear boundary in the frequency-bandwidth data space normally represent an actual constant signal. This phenomenon is in line with the clustering hypothesis proposed by the authors in [56]. They stated that in the fast density-based clustering method (FDP), the center data point of a cluster usually has a higher density than its surrounding data points and relatively large distances from other cluster centers.

In accordance with the FDP method, a basic clustering strategy is formed for dense grids. We initially treat the SFVs in all dense grids as a whole area. Then, we distinguish the SFVs that can be regarded as cluster centers. Lastly, we classify the other SFVs into the nearest cluster center to complete the clustering. Notably, this process has two key points. The first point is that the FDP method measures the density of an SFV by calculating the number of SFVs within its cutoff distance  $dc$ . Such density measurement is sensitive to the setting of  $dc$ . The second point is that the FDP method does not provide a quantitative method for determining the number of cluster centers.

For density measurement, we propose to use the  $K$ -nearest neighbor kernel density [64]. We first find the  $K$ -nearest SFVs to the current examined SFV  $i$ . Then, we calculate their density using a kernel density function. The local density  $\rho(i)$  is defined as

$$\rho(i) = \frac{\sum_{j \in K(i)} \exp(-d(i, j))}{k}, \quad (2)$$

where  $k$  is usually the value  $\sqrt{N}$ ,  $K(i)$  is the  $K$ -nearest neighbors of SFV  $i$ , and  $d(i, j)$  represents the Euclidean distance between SFVs  $i$  and  $j$ . This density can be accurately estimated because the fixed  $dc$ -distance is discarded, and it can be efficiently calculated because only a few neighbor SFVs are involved in the computation.

To determine the number of cluster centers automatically, we apply the relative density proposed in [34]. Our basic idea is that if an SFV is a cluster center, then no SFV whose density and minimum distance are larger than those of the cluster center SFV exists in its  $K$ -nearest neighbors. That is, the SFV's local relative density and local relative minimum distance in its  $K$ -nearest neighbors should be equal to 1. We define the local relative density  $\rho^*(i)$  and relative minimum distance measure  $\delta^*(i)$  of SFV  $i$  as

$$\rho^*(i) = \frac{\rho(i)}{\max_{j \in K(i) \cup \{i\}} \{\rho(j)\}}, \quad \delta^*(i) = \frac{\delta(i)}{\max_{j \in K(i) \cup \{i\}} \{\delta(j)\}}, \quad (3)$$

where  $\delta(i) = \min_{j: \rho(j) > \rho(i)} d(i, j)$ .

We regard SFV  $i$  as a cluster center when  $\rho^*(i) = 1$  and  $\delta^*(i) = 1$ . After traversing all SFVs, we obtain many SFVs whose number is exactly the number of cluster centers.

### 5.1.3 Sparse Area Processing

Sparse grids are commonly ignored in many grid-based clustering methods, but this is not the case in signal clustering. On one hand, several SFVs in sparse grids may be boundary SFVs that belong to the clusters of adjacent dense grids. On the other hand, periodic short-term signals may exist in sparse grids. These signals appear periodically and transiently. They usually contain a certain number of SFVs that are less than a constant signal but more than an instantaneous signal. Therefore, it is possible to distinguish these signals in the signal clustering.

In terms of possible cluster boundary SFVs, for each SFV in sparse grids, we calculate the distances from the SFV to all cluster centers in its adjacent dense grids. The SFV is assigned to the corresponding cluster when the distance is less than the grid width. Regarding periodic short-term signals, for each sparse grid, we initially use the clustering method of the dense area to process the SFVs. Then, we observe the SFVs' time distribution in each obtained cluster. A cluster can be regarded as a periodic short-term signal when the SFVs of this cluster cover most of the monitored period. Otherwise, all SFVs of this cluster are considered noises. We use an empirical value of 80% for this time span ratio.

### 5.1.4 Interference Processing

Several SFVs in a cluster may have low strength or SNR values. This condition commonly indicates that a signal, especially a constant one, is disturbed by environmental noises or unknown signals, thereby leading to poor communication quality or even temporary interruption. Therefore, we conduct an interference process to re-examine the strength and SNR values of the SFVs in the obtained clusters. If the strength or SNR of an SFV is below the strength threshold or the SNR threshold set by users, then the SFV is treated as a noise. This process can facilitate the detection of short-time interruptions or instability of constant signals.

### 5.1.5 Authorized Signal Inspection

When users have an authorized signal library that records the major registered radio signals allowed for lawful communication, this step must be performed so that the obtained signals match the library signals in terms of time, center frequency, and bandwidth. If an obtained signal already exists in the library, then it is an authorized signal. Otherwise, it is unauthorized and should be heeded by users for further analysis.

## 5.2 Situation Assessment

Electromagnetic situation awareness is immensely complex and challenging (C3). In many sophisticated applications introduced in subsection 2.2, objective situation assessment and human-in-loop interactive analysis are well combined to achieve situation awareness. On this basis, we propose a situation assessment model based on SigData and signal clustering results to provide quantitative and qualitative electromagnetic situation descriptions. This model is expected to reduce users' cognitive load and domain-experience requirements in situation assessment and facilitate the subsequent situation analysis. The assessment index system and situation-level generation of the model are described in detail below.

### 5.2.1 Assessment Index System

We design a multi-index system by considering various influencing factors formulated from domain knowledge and expert experience. Each index represents a situational factor and all indexes are combined to describe an overall electromagnetic situation. A time interval and a given frequency band are essential for real-time situation monitoring. In this work, we use a 10s time interval and a frequency unit of 1 MHz by default. In other words, the entire band is equally divided into 1 MHz sub-bands. For each sub-band, we design 12 situation indexes that can be classified into indexes for all signals (AL), authorized signals (AU), unauthorized signals (UN), and noise (NO) from the perspective of signal types. They can also be categorized into indexes for frequency domain (FRE), time domain (TIM), and energy domain (STR) in terms of signal characteristics. These indexes form a hierarchical tree structure that conjointly describes the situation of a 1 MHz sub-band in 10s. Moreover, the index system is an experience-based textual description. The quantitative situation values of these indexes need to be calculated by introducing diverse computational analysis methods. The specific calculation methods of the 12 indexes are provided in the supplementary material of this paper.

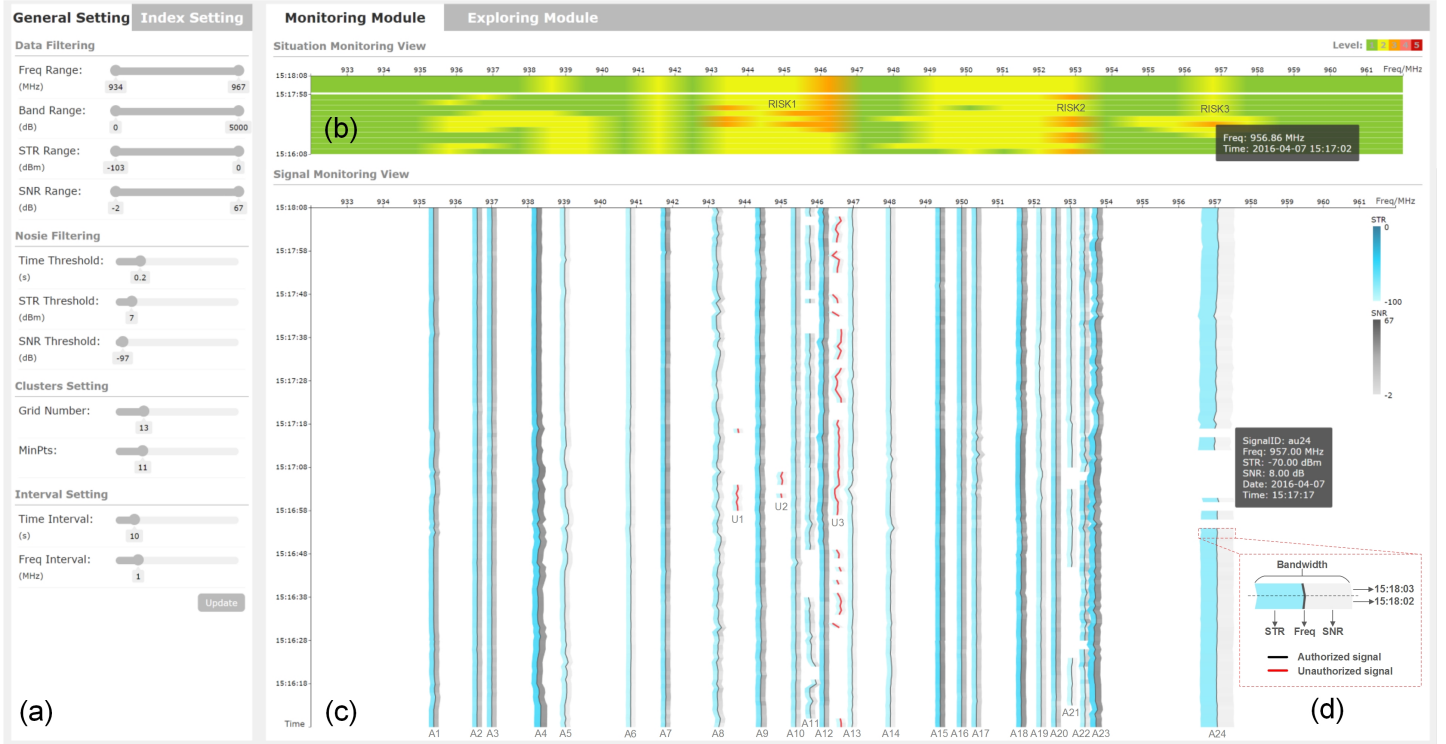


Figure 4. System interface consists of a control panel (a) and two functional modules. The monitoring module provides a situation monitoring view (b) and a signal monitoring view (c) to help users achieve situation perception. The situation monitoring view (b) presents an overview of the current electromagnetic situation and its recent change trend. The signal monitoring view (c) uses an STF diagram with a river visualization mode to depict the signal distribution in time and frequency and the time-varying patterns of the signals' characteristics. Its visual encoding is illustrated in (d).

## 5.2.2 Situation-level Generation

Situation-level generation transforms calculated quantitative index values into readable qualitative situation levels. Referring to [75], we use a three-step method to generate situation levels. (1) We define five levels of the electromagnetic situation of a sub-band in a period on the basis of the partition method of American National Security Level. The five levels are expressed as dimensionless points from 1 to 5, [1 = low, 2 = guarded, 3 = elevated, 4 = high, 5 = severe]. (2) For an individual index, we initially use a trapezoidal fuzzy membership function [10, 75] to transform a situation value into a fuzzy membership vector belonging to the five situation levels by combining the thresholds provided by users. Then, we select the maximum degree of the fuzzy membership vector as the situation level of the index. (3) For the assessment index system, we construct a fuzzy relation matrix to generate a weighted fuzzy membership vector in accordance with the weights of the 12 indexes provided by users. Then, we select the maximum membership degree from the weighted vector as the overall situation level of the index system.

## 6 INTERFACE AND INTERACTION

### 6.1 Interface

We design a system interface with two visual analysis modules, namely, monitoring and exploring modules, to support users' daily work. The major consideration is that users' daily work has two operation modes: monitoring and exploring. The two modes have different requirements in data presentation and interactive analysis. In the monitoring mode, users are required to observe the current electromagnetic situation. Thus, an intuitive and up-to-date presentation of necessary information related to the overall situation and signal distribution is required. Users switch to the exploring mode when any abnormal clue is observed. In this mode, they need to analyze relevant SigData and SpeData carefully for in-depth understanding. The interface at this time should present rich contextual information from multiple perspectives and support flexible interactions. This design can avoid stacking excessive information in one interface and can support dual-screen display with necessary software and hardware.

### 6.1.1 Monitoring Module

The monitoring module helps users perceive the overall electromagnetic situation (R3) and the integral distribution of radio signals in the monitoring frequency band (R4). This module consists of a situation monitoring view that visualizes the results of situation assessment in the latest period and a signal monitoring view that visualizes the results of signal clustering in the same period. The two views are periodically animated to support the continuous monitoring and inspection with a default update interval of 10s. Many design considerations and design alternatives are detailed in the supplementary material of this paper.

**Situation monitoring view** adopts the design idea of level-progressive heatmap to present an overview of the current electromagnetic situation and its recent change trend (Figure 4(b)). The design is manifested from two aspects, namely, gradual progresses in time and frequency.

The current situation is what users are most concerned about. Users wish to observe recent situation changes simultaneously (e.g., usually in the last 2–3min). We divide the y-axis timeline of the view into two levels, namely, major and auxiliary. The major level occupies a large vertical space at the top of the y-axis to show the current situation. The remaining y-axis space is evenly divided into 10 small segments to display the recent situations as the auxiliary level. The default setting of the time interval of a segment is 10s. Hence, the current situation can be easily perceived in the major level. Continuous small segments in the auxiliary level use a limited vertical screen space to reveal the situation's change trend.

Users wish to highlight high-risk frequency sub-bands. We equally divide this view's x-axis that represents the monitoring band into cells from left to right. A cell represents a frequency sub-band with a default interval of 1 MHz. The color of a cell represents the situation level of the relevant sub-band generated by situation assessment. Colors are encoded with five levels following the rule that a high risk is presented in a vibrant color. We also use a linear interpolation to handle the color transition between cells. This interpolation represents the possible uncertainty of situation level in the boundary frequencies among adjacent sub-bands. Overall, this view provides an intuitive heatmap-based visualization with rich levels of details on time and frequency.

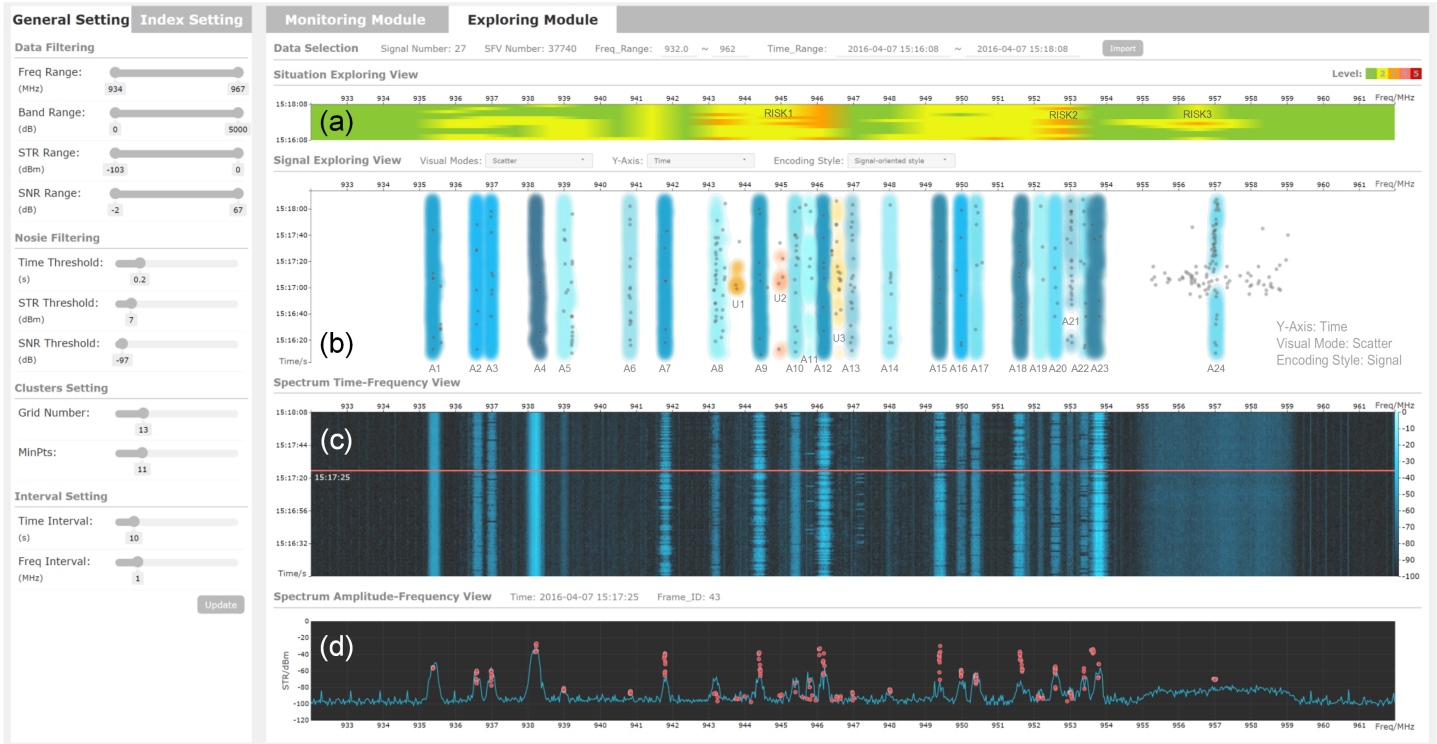


Figure 5. Exploring module provides four coordinated visualization views to help users achieve situation understanding. The situation exploring view (a) provides the situation information of the explored time period and frequency band. The signal exploring view (b) uses an STF diagram with a scatter visualization mode to support a multi-perspective and interactive SigData exploration. The spectrum time-frequency view (c) and spectrum amplitude-frequency view (d) present the corresponding SpeData to facilitate a joint analysis of SigData and SpeData for high-risk situation understanding.

**Signal monitoring view** depicts the distribution of all signals in time and frequency as well as the time-varying patterns of the signals' characteristics. As stated in C2, this view involves two design challenges, namely, (1) how to produce a continuous distribution visualization by using characterized and discretized SigData and (2) how to present the time-varying patterns of a signal's four basic characteristics simultaneously.

Inspired by a river metaphor [5, 26, 40, 43], we create a new signal time-frequency (STF) diagram to address the two design challenges (Figure 4(c)). The diagram's  $x$ -axis shows the monitored frequencies from left to right, and the  $y$ -axis represents the time period consistent with the situation view from top to bottom. This layout is commonly used in the spectrum time-frequency diagram, which our target users are accustomed to. Inside the diagram are ribbon-like rivers, each of which represents a radio signal obtained through signal clustering. The number of these ribbon-like rivers indicates how many signals are in communication. A river is composed of a series of quadrilaterals sequentially arranged along with time. A quadrilateral encodes the four means of four basic characteristics of the SFVs of a signal in a time span with a default interval of 1s.

As shown in Figure 4(d), for a quadrilateral in a river, the  $x$ -axis position of its center line represents the mean of center frequency. The width represents the mean of bandwidth. The color of its left sub-area divided by the center line represents the mean of signal strength, and the color of its right sub-area represents the mean of SNR. For the colors of the two sub-areas, the more saturated the color is, the larger the corresponding value is. Moreover, a time interruption may occur in the corresponding river if a signal does not have sufficient SFVs (five by default) within a time span. The center line of the corresponding river of a signal is highlighted in red color when it is a newly found unauthorized signal.

In short, the river visualization design of the STF diagram can roughly depict the continuous distribution of all radio signals in time and frequency from a global view. It can present the time-varying patterns of a signal's four basic characteristics from a local view. Moreover, it fits users' mental map well because the river metaphor provides a similar visual perception experience as the spectrum time-frequency diagram commonly used in SpeData analysis.

## 6.1.2 Exploring Module

The exploring module aims to help users determine the root causes of communication anomalies and understand high-risk situations (R5). To provide rich contextual information, one information bar and four visualization views are designed in this module to present SigData and SpeData from multiple perspectives. The information bar at the top of this module describes the time period and frequency band being investigated, the number of SFVs in the original SigData, and the number of signals discovered by signal clustering. The four visualization views occupy the majority of the area of this view from top to bottom, with a compact and vertical layout. To facilitate a joint and comparative analysis, all four views use frequency as the  $x$ -axis and focus the data exploration on the same range of time and frequency.

**Situation exploring view** shows the situation information of the currently explored time period and frequency band (Figure 5(a)). Its visualization design is roughly similar to the situation monitoring view in the monitoring module, except that its time  $y$ -axis is not level progressive.

**Signal exploring view** is the major view in this module for interactive analysis of SigData (Figure 5(b)). An STF diagram is still used in this view. However, a new visualization mode (scatter mode) and additional interactions are provided. The scatter mode visualizes SigData via a scatterplot, in which a dot represents an SFV. This mode supports multi-perspective visualization of SigData. First, its  $y$ -axis can switch to time, bandwidth, strength, or SNR depending on the users' analytical requirements. Second, this mode provides three encoding styles, namely, full, signal-oriented, and noise-oriented styles. The three encoding styles are introduced as follows.

The full style displays all SFVs of SigData in the currently investigated time period and frequency band. In Figure 6(a), dots with the same color are SFVs that belong to the same cluster classified by signal clustering. The gray dots are noise SFVs identified by signal clustering. This style shows all SFVs at the same time, but it often suffers from severe visual clutter because of the overlapping of noise and normal SFVs.

The signal-oriented style highlights SFV clusters and reduces the impact of noise SFVs on cluster observation. In Figure 5(b) and Figure 6(b), an SFV cluster, also called a signal, is represented by an ellipse with a light gray contour and a gradient inner color. The contour is generated by

applying marching squares, and the gradient inner color is obtained based on the SFV density distribution of the cluster estimated through kernel density estimation. For noise SFVs, we use a random sampling with a 10% default sampling rate to reduce the number of noise SFVs displayed in the scatter. The reserved noise SFVs are drawn with gray dots, roughly depicting the noise distribution.

The noise-oriented style is designed to help users analyze the impacts of noise SFVs on radio communication. In this style, SFV clusters are represented by transparent areas with gray contours, as shown in Figure 6(c). Meanwhile, noise SFVs without sampling are represented by red dots to highlight the noise distribution. The higher the transparency of a dot is, the higher the strength of the noise SFV is.



Figure 6. Three encoding styles of the STF diagram with the scatter visualization mode: (a) full style where the  $x$ -axis is the frequency and the  $y$ -axis is the bandwidth, (b) signal-oriented style where the  $x$ -axis is the frequency and the  $y$ -axis is the bandwidth, and (c) noise-oriented style where the  $x$ -axis is the frequency and the  $y$ -axis is the time. The scatter mode allows users to set the dimension shown on the  $y$ -axis.

**Spectrum time-frequency view and spectrum amplitude-frequency view** are for the joint analysis of SigData and SpeData in this module (Figure 5(c–d)). SpeData is a primitive data source in RMM. It facilitates situation understanding and performs well in the verification of signal clustering results. The two views are designed based on traditional spectrum time-frequency and amplitude-frequency diagrams. The time-frequency view shows all spectrum frames in SpeData. The  $y$ -axis displays the time (i.e., the frame number) from top to bottom. The  $x$ -axis uses small and dense color dots to show the signal amplitudes of all the frequencies in a frame from left to right. The brighter the color is, the larger the amplitude is. The amplitude-frequency view, whose  $x$ -axis is the frequency and  $y$ -axis is the amplitude, uses a line chart to visualize the amplitude variation of a frame in frequency, and it also employs a scatterplot to present the SFVs in SigData corresponding to the frame. This design allows users to directly compare the two kinds of data in a single view. In addition, the two views use a dark background. This condition meets users’ habits of observing SpeData and distinguishes the two views from the white background adopted by the views showing SigData.

## 6.2 Interaction

The system features a set of interactions to help users easily and effectively conduct situation monitoring and data exploration (R6).

**Detail on demand.** Detailed information appears when users move or click the mouse in each view. Moreover, each view can zoom in and out of the frequency axis by scrolling the mouse wheel. The signal exploring view provides users with rich visualization options (e.g., view modes and encoding styles) for flexible data exploration.

**View updating.** The system supports two view updating manners. Automatic updating occurs in the monitoring module to display the latest situation and signal information. Coordinated updating occurs in the views in the same module via interactions. For example, in the exploring module, users can select a frame in the time-frequency view to observe its detailed amplitudes in the amplitude-frequency view.

**Module connection.** In the monitoring module, users can draw a rectangle in the situation monitoring view or signal monitoring view to select

the high-risk sub-bands or signals of interest. After double-clicking the rectangle, the relevant SigData and SpeData are loaded into the exploring module for the subsequent analysis.

**Interactive adjustment of clustering results.** The signal exploring view provides signal merging and signal splitting interactions to help users adjust the signal clustering results. The signal merging interaction enables users to merge two signals into one on the basis of their observation of the clustering results and corresponding SpeData. The signal splitting interaction enables users to mark a group of selected SFVs as a new signal.

**Parameter settings.** The system provides a control panel to allow users to set the parameters required for system operations, as shown in Figure 4(a). These parameters primarily include the parameters of signal clustering, the situation updating time interval, the frequency interval of situation calculation, and the weight of each situation assessment index.

## 7 EVALUATION

We evaluated the system through a signal clustering experiment, a case study and a user interview. The entire evaluation process was accomplished in collaboration with two target users, namely, a manager and a radio supervisor in a radio administration bureau, who can provide professional insights into data analysis.

### 7.1 Signal Clustering Experiment

We used two real-world SigData sets to verify the effectiveness of the proposed signal clustering method. The first set (SData1) is the SigData in the band of 930–965 MHz collected from 15:11:08 to 15:30:22 on April 7, 2016, with an average of 403 SFVs per second. The second set (SData2) is the SigData in the band of 935–955 MHz collected from 11:28:10 to 12:11:29 on July 5, 2016, with an average of 257 SFVs per second. To obtain the ground truth of signal clustering, we invited the two users to perform manual signal identification. Considering the scenario of real-time monitoring, our experiment was conducted at 10s and 60s time intervals, which are often used in actual work. With SData1 and 10s interval as an example, we performed signal clustering for 116 times on SData1 as its time span is 1154s. We used DBSCAN and FDP as the reference algorithms in our comparative analysis. DBSCAN and FDP are important methods that we referred to when designing our method. In DBSCAN, the parameter  $Eps$  was determined with the method in [33, 46], and the parameter  $MinPts$  used the empirical value of 4. In FDP, the parameter  $dc$  was set through empirical experience (i.e., the distance  $d_{ij}$  between all SFVs was arranged in an ascending order and the first 2% was used as the  $dc$  value), and the number of clustering centers was determined according to the signal numbers obtained by our method. We collected the accuracy and recall rates of each clustering and used the average accuracy and recall rates as our experimental result.

The experimental result (Table 1) showed that our clustering method performed better than DBSCAN and FDP in terms of average accuracy and recall rates. With regard to average time, DBSCAN was time consuming because of the calculation complexity of  $Eps$ , whereas our method presented a high running efficiency. FDP had a low running time, but the time spent on manually determining the number of clustering centers was not counted in the experiment. With regard to the data quantity of the two experiment data sets, our method only required 1–2s and 4–5s for 10s and 60s intervals, respectively. Overall, our method achieved a good efficiency and accuracy, and met the requirements of real-time situation monitoring on the two data sets.

Table 1. Result of the signal clustering experiment

Data	Interval	Avg precision			Avg recall			Avg time (s)		
		DBSCAN	FDP	Ours	DBSCAN	FDP	Ours	DBSCAN	FDP	Ours
SData1	10s	0.80	0.85	0.91	0.81	0.78	0.94	42.89	1.12	1.31
	60s	0.76	0.81	0.85	0.78	0.79	0.93	276.21	5.46	5.03
SData2	10s	0.76	0.81	0.87	0.80	0.83	0.89	30.67	0.87	0.95
	60s	0.79	0.83	0.88	0.79	0.82	0.91	195.34	4.34	4.16

Moreover, our method identified a small number of signals that were not included in the ground truth (see the analysis of RISK1 and RISK2 in the case study). The users confirmed that the signals could not be easily distinguished through manual SpeData observation. In addition, our

prototype system allowed the interactive verification and adjustment of automatic clustering results (see the analysis of RISK2 in the case study).

## 7.2 Case Study

Our case study used SData1 whose frequency band (932–962 MHz) is at microwave frequencies and can be used for Global System for Mobile Communication (GSM). The monitoring moment was 15:18:08 on April 7, 2016, and the situation updating interval was set to 10s. The frequency unit of situation calculation was 1 MHz. The weights of the indexes ALL\_FRE\_OPY (All signals' frequency occupancy) and NO\_PER (the proportion of noise SFVs to all SFVs) were set to 0.1, the weights of the five AU indexes were set to 0.075, and the weights of the five UN indexes were set to 0.085.

**Perception of the overall situation and signal time-frequency distribution.** The first step in the case study was to perceive the overall situation and the distribution of detected radio signals in the monitoring module. The situation monitoring view in Figure 4(b) intuitively presents the current situation and its changes in the last 2min, during which the entire band had a superior overall situation and a relatively stable trend. However, three sub-bands, namely, 943–947 MHz (RISK1), 952–954 MHz (RISK2), and 956–958 MHz (RISK3), had high-risk situation levels. The STF diagram in the signal monitoring view uses the river visualization mode to clearly depict the time-frequency distribution and time-varying patterns of all radio signals, as shown in Figure 4(c). Several interesting clues related to the three risks can be found in the STF diagram. In the sub-bands around RISK1, three unauthorized signals, namely, U1, U2, and U3, were intermittent and had very low SNR values. Around RISK2, we found that the authorized signal A23 had a swinging center frequency and a slight overlap with its nearest signal. Around RISK3, the authorized signal A24 had the largest bandwidth in the band and a stable center frequency, but its strength and SNR were low. An obvious communication interruption lasting for 30s occurred around 15:17:00 on this signal. To determine the root causes of the three risks and gain an in-depth situation understanding, we selected the three relevant sub-bands as research objects in conducting a detailed data exploration in the exploring module in the subsequent steps.

**Situation understanding of RISK1.** We analyzed the RISK1-related SigData and SpeData (943–947 MHz and 15:16:28 to 15:18:08) in the exploring module. We set the STF diagram in the signal exploring view with the scatter visualization mode and the full style where the  $x$ -axis is the frequency and the  $y$ -axis is the SNR. As shown in Figure 7(a), three unauthorized signals were marked with U1, U2, and U3, respectively. All SFVs of the three signals had low SNR values and were almost covered by a large number of gray-noise SFVs. We observed the spectrum time-frequency view (Figure 7(b)). Most of the authorized signals were clearly presented by bright vertical ribbons. However, no obvious ribbon was observed at the frequencies of the three unauthorized signals. We further observed the spectrum amplitude-frequency view (Figure 7(c)). The amplitudes at the frequencies of the three signals were low. All of the above visualization results validated the low strength/SNR features of the three unauthorized signals. The users stated that such weak signals were difficult to identify via manual observation of SpeData in traditional spectrum diagrams. They also confirmed that the use of SigData and the prototype system could help them identify the existence of weak signals and the impact of these signals.

**Situation understanding of RISK2.** We analyzed the RISK2-related SigData and SpeData (952–954 MHz and 15:16:28 to 15:17:58) in the exploring module. We first set the STF diagram in the signal exploring view with the signal-oriented style where the  $x$ -axis is the frequency and the  $y$ -axis is the bandwidth. As shown in Figure 8(a), the authorized signal A23 had two SFV clusters marked as A23-1 and A23-2. The two sub-signals had completely different center frequencies and bandwidths. We then switched the  $y$ -axis of this view to time (Figure 8(b)). The two sub-signals lasted for the entire time period. We further observed the spectrum time-frequency view (Figure 8(c)). Two bright overlapping ribbons were noted at the frequencies of A23-1 and A23-2. The users explained that the series of visualization results demonstrated that the A23 signal might be an unstable frequency division multiplexing signal. Frequency division multiplexing (FDM) technology has an inherent defect, that is, the amplifiers used by FDM signals may show nonlinear distortion, thereby leading to signal overlap and inter-channel interference. The users



Figure 7. Situation understanding of RISK1. (a) Three unauthorized signals (U1, U2, and U3) with low SNR values are found. (b) No clear bright vertical ribbon is observed at the frequencies of U1–U3. (c) The spectrum amplitudes at the frequencies of U1–U3 are very low.

suggested that the A23-1 and A23-2 sub-signals can be regarded as two separate signals for completing the same communication task. We therefore selected the SFVs in the A23-2 sub-signal and performed a signal splitting operation to interactively adjust the signal clustering result. As shown in Figure 8(d), the original A23-2 sub-signal was marked as A25 with a different color. The users confirmed that our signal clustering method can identify the multiplexing signal, and our situation model can indicate the instability of the signal.

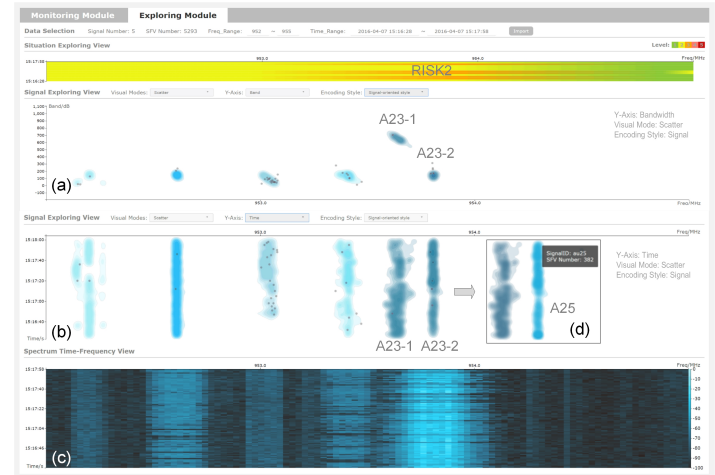


Figure 8. Situation understanding of RISK2. (a) Two sub-signals of authorized signal A23 are found. (b) The two sub-signals last for the entire time period. (c) Two bright ribbons at the frequencies of A23-1 and A23-2 overlap. (d) A23-2 is interactively set as a separated signal by using a signal splitting interaction.

**Situation understanding of RISK3.** As shown in the signal exploring view with the noise-oriented style in Figure 6(c), a large number of noise SFVs highlighted with red points suddenly appeared in the sub-band 956–958 MHz from 15:16:48 to 15:17:18. These noise SFVs had a wide distribution in frequency. The users explained that a strong noise interference should be responsible for RISK3, which affected the communication of the authorized signal A24 and even led to its short communication interruption.

## 7.3 User Interview

We conducted a user interview with the manager and supervisor after they viewed our demonstration and tried out the prototype system. We asked several questions during the interview. The feedback on each question are detailed as follows.

**Q1: Are you satisfied with the signal clustering method?** Both target users were generally satisfied with the proposed signal clustering method. *“Overall, the method is accurate and efficient. I am particularly satisfied with the using of time, signal strength, and SNR in this method.”* The manager commented, *“Traditional methods generally only consider center frequency and bandwidth for clustering, which cannot bring about ideal results in complex scenarios.”* The supervisor said, *“This method seems potent to address the problem of uneven signal distribution. And I like the immediate visualization and interactive adjustment of clustering results.”*

**Q2: Are you satisfied with the situation assessment model?** The users confirmed that the situation assessment model was devised by considering their experience. According to the manager, *“This attempt has two praiseworthy points: one is to verify the feasibility of using signal data in daily work. The other is to demonstrate the important role of visual analysis in situation awareness.”* The supervisor added, *“I appreciate the model provides rich settings and a flexible structure for adding new indexes. And the qualitative processing is impressive. It facilitates visual situation perception and enhances the operability of the assessment model.”*

**Q3: Is the interface intuitive and easy to use?** The users agreed that the visualizations and interactions were carefully designed to fit their mental maps and operation habits. *“Overall, the interface looks very intuitive and comfortable.”* According to the supervisor, *“I believe most supervisors can get started quickly.”* The manager praised, *“This two-module interface is thoughtful and in line with our daily work.”*

**Q4: Is the interface informative and helpful?** The users confirmed that the interface was informative and helpful. *“Signal river visualization is very impressive. It significantly improves the abilities of information presentation and interactive analysis of traditional spectrum time-frequency diagram.”* The manager commented, *“I look forward to seeing this visualization become a standard tool for interactive signal data analysis.”* The supervisor affirmed that the situation visualization will definitely improve their working efficiency, especially for those new supervisors without much experience. The manager appreciated that we provided a joint analysis environment for SigData and SpeData. He said, *“This is exactly what I want, the complementarity and mutual verification of these two kinds of data in actual work are very necessary.”*

**Q5: Which part can be further improved?** We encouraged the target users to give improvement suggestions. For the interface, they suggested that the system should provide the viewing functions of raw data and authorized signal library. The manager suggested, *“Signal data may have more data fields, such as modulation type and geographic information.”* Regarding the signal clustering method, the manager commented, *“Actually, signal data can be seen as the result of signal clustering on spectrum data. Now since your signal clustering takes a step further, we need to consider the possibility of integrated multi-stage clustering.”*

**Q6: How much are you looking forward to this system?** The target users encouraged us to continue improving this prototype system. The manager confirmed that they will try our prototype system. They will also cooperate with us to involve more staff to perform an in-depth user study. Looking ahead to the future, the manager said, *“This study boosts our confidence to apply signal data and visual analysis technologies in radio monitoring and management.”* He added, *“I hope you can address more challenging problems, such as a wide frequency band and a large data scale, particularly complex signals like frequency hopping/spread/multiplexing signals, and newer communication technologies like 4G and even 5G.”*

## 8 DISCUSSION

In this section, we discuss the limitations and future work of this study.

We discuss the potential scalability issue of our visualization design on frequency and time domains. For frequency visualization, we mainly consider the following two aspects. (1) Spectrum sensing equipment have a core component called digital down converter (DDC), which is responsible for translating radio signals from high frequencies (e.g., GHz) to intermediate frequencies (e.g., MHz) in order to simplify the subsequent processing stages (e.g., amplification and demodulation). Generally, the real-time processing capability of a DDC is limited to a certain bandwidth (e.g., 36 MHz). (2) Our scenario focuses on monitoring important signals in real time and maintaining their normal communication within a certain area. Most voice and video communication signals occupy a relatively narrow frequency band of less than 50 MHz. For example, a GSM signal

occupies a maximum of 30 MHz frequency band. In our case study, the monitoring band ranged from 932–962 MHz, which fully covered our target GSM signal. In terms of time visualization, our target users confirmed that showing the relevant data within the recent 2–3min is sufficient to make a quick decision in their daily work. To sum up, the proposed visualization design of frequency and time domains is in line with the users’ requirements. The interface does not often encounter the serious issue of visual scalability in the target scenario. However, our target users stated that many scenarios are required for the analysis of long-term data and wide frequency bands in RMM. The interface would certainly encounter serious visual clutter if it is directly applied to such scenarios. A potential solution is to design a hierarchical visual analysis framework.

Several parameters of the proposed signal clustering method and situation assessment model are currently set based on our experimental experience. Although users can interactively adjust these parameters, this process remains a potential problem in practical use. We plan to try intelligent recommendation methods to assist users in setting optimal parameters. Moreover, the clustering method currently performs well in constant signal identification. However, it still needs to be improved when it is applied to complex signals, such as frequency hopping, spread spectrum, and time division multiplexing signals. This improvement may require the integration of information from SpeData.

The color encoding of the signal exploring view is a bit difficult to decide (Figure 5(b)). The common manner of visualizing a clustering result is to encode the clusters with different colors. However, many clusters/signals are to be shown in this view. This view will become cluttered if the colors of the clusters are highly differentiated. Therefore, we provide two options for users to choose from based on their preferences. The first option is to encode the authorized signals with cool colors and the unauthorized signals with warm colors. The second option is to encode all signals with the same color, as shown in Figure 6(c).

The interface can also be further improved. We plan to design a functional view to visualize the specific calculated values of situation assessment indexes. In this way, the interface can construct a three-level visualization mode that supports the integral risk analysis from the situation levels to the situation indexes and then to the relevant SpeData and SigData. In addition, we plan to add other features to the interface, such as viewing functions for raw data and an AU signal library. Moreover, although the users affirmed the practical value of our approach, the level of aid that our approach can provide to actual work remains unclear. We need to conduct further user studies and evaluation verifications.

## 9 CONCLUSION

This study proposed an improved clustering method based on DBSCAN and FDP to process SigData, a novel STF diagram for the interactive exploration of radio signals, and a visual analysis prototype system for assessing, perceiving, and understanding electromagnetic situations. Evaluations on real-world data sets and an interview with actual users were conducted to verify the effectiveness of the proposed visual analysis prototype system. This study is a preliminary attempt to introduce visual analysis technologies into electromagnetic situation awareness. This work also demonstrates the usability of conducting a joint analysis of SigData and SpeData for RMM. We hope that the visualization and interaction design of the STF diagram can fulfill similar interactive analysis tasks of time-varying multidimensional data in other scenarios. We also hope that our situation awareness solution will inspire a wide range of relevant studies and applications.

## ACKNOWLEDGMENTS

We wish to thank all the anonymous reviewers for their valuable comments. The work is supported in part by the National Key Research and Development Program of China (No. 2018YFB1700403), the National Natural Science & Technology Fundamental Resources Investigation Program of China (No. 2018FY10090002), the National Natural Science Foundation of China (No. 61872388, 61772456, 61761136020, 61672538, and 61502540), the National Science Foundation of Hunan Province (No. 2019JJ40406), the Open Project Program of the State Key Lab of CAD & CG, Zhejiang University (No. A1902), and the Open Research Fund of Beijing Key Laboratory of Big Data Technology for Food Safety, Beijing Technology and Business University (No. BKBD-2018KF08).

## REFERENCES

- [1] Architecture of radio. <http://www.architectureofradio.com>. Accessed: 14-January-2019.
- [2] The homepage of rohde & schwarz. <http://www.rohde-schwarz.com.cn>. Accessed: 6-February-2019.
- [3] The homepage of tektronix. <https://www.tek.com.cn>. Accessed: 22-January-2019.
- [4] A. A. Adnani, J. Duplity, and L. Philips. Spectrum analyzers today and tomorrow: part 1 towards filterbanks-enabled real-time spectrum analysis. *IEEE Instrumentation Measurement Magazine*, 16(5):6–11, Oct 2013. doi: 10.1109/MIM.2013.6616284
- [5] W. Aigner, S. Miksch, W. Miller, H. Schumann, and C. Tominski. Visual methods for analyzing time-oriented data. *IEEE Transactions on Visualization and Computer Graphics*, 14(1):47–60, Jan 2008. doi: 10.1109/TVCG.2007.70415
- [6] A. Ali and W. Hamouda. Advances on spectrum sensing for cognitive radio networks: theory and applications. *IEEE Communications Surveys and Tutorials*, 19(2):1277–1304, May 2017. doi: 10.1109/COMST.2016.2631080
- [7] M. Angelini, G. Blasilli, T. Catarci, S. Lenti, and G. Santucci. Vulnus: Visual vulnerability analysis for network security. *IEEE Transactions on Visualization and Computer Graphics*, 25(1):183–192, Jan 2019. doi: 10.1109/TVCG.2018.2865028
- [8] G. Arthur Van, F. Staals, M. Lffler, J. Dykes, and B. Speckmann. Multi-granular trend detection for time-series analysis. *IEEE Transactions on Visualization and Computer Graphics*, 23(1):661–670, Jan 2017. doi: 10.1109/TVCG.2016.2598619
- [9] P. Baltiiski, I. Iliev, B. Kehaiov, V. Poulkov, and T. Cooklev. Long-term spectrum monitoring with big data analysis and machine learning for cloud-based radio access networks. *Wireless Personal Communications*, 87(3):815–835, Apr 2016. doi: 10.1007/s11277-015-2631-8
- [10] A. Barua, L. S. Mudunuri, and O. Kosheleva. Why trapezoidal and triangular membership functions work so well: Towards a theoretical explanation. *Journal of Uncertain Systems*, 8(3):164–168, 2014.
- [11] M. Behrisch, D. Streeb, F. Stoffel, D. Seebacher, B. Matejek, S. H. Weber, S. Mittelstaedt, H. Pfister, and D. Keim. Commercial visual analytics systems—advances in the big data analytics field. *IEEE Transactions on Visualization and Computer Graphics*, Jul 2018. doi: 10.1109/TVCG.2018.2859973
- [12] T. Blascheck, L. M. Vermeulen, J. Vermeulen, C. Perin, W. Willett, T. Ertl, and S. Carpendale. Exploration strategies for discovery of interactivity in visualizations. *IEEE Transactions on Visualization and Computer Graphics*, 25(2):1407–1420, Feb 2019. doi: 10.1109/TVCG.2018.2802520
- [13] M. Brehmer, B. Lee, B. Bach, N. H. Riche, and T. Munzner. Timelines revisited: A design space and considerations for expressive storytelling. *IEEE Transactions on Visualization and Computer Graphics*, 23(9):2151–2164, Sep. 2017. doi: 10.1109/TVCG.2016.2614803
- [14] L. Byron and M. Wattenberg. Stacked graphs-geometry & aesthetics. *IEEE Transactions on Visualization and Computer Graphics*, 14(6):1245–1252, Nov 2008. doi: 10.1109/TVCG.2008.166
- [15] A. Cantu, T. Duval, O. Grisvard, and G. Coppin. Helovis: A helical visualization for sigint analysis using 3d immersion. In *Proceedings of the 2018 IEEE Pacific Visualization Symposium (PacificVis)*, pp. 175–179. IEEE, Apr 2018. doi: 10.1109/PacificVis.2018.00030
- [16] N. Cao, C. Shi, S. Lin, J. Lu, Y. Lin, and C. Lin. Targetvue: Visual analysis of anomalous user behaviors in online communication systems. *IEEE Transactions on Visualization and Computer Graphics*, 22(1):280–289, Jan 2016. doi: 10.1109/TVCG.2015.2467196
- [17] D. Chen, J. Yang, J. Wu, H. Tang, and M. Huang. Spectrum occupancy analysis based on radio monitoring network. In *Proceedings of the 2012 1st IEEE International Conference on Communications in China: Wireless Networking and Applications (WNA)*, pp. 739–744. IEEE, Aug 2012. doi: 10.1109/ICCChina.2012.6356981
- [18] Q. Chen, Y. Chen, D. Liu, C. Shi, Y. Wu, and H. Qu. Peakvizor: Visual analytics of peaks in video clickstreams from massive open online courses. *IEEE Transactions on Visualization and Computer Graphics*, 22(10):2315–2330, Oct 2016. doi: 10.1109/TVCG.2015.2505305
- [19] S. Chen, J. Li, G. Andrienko, N. Andrienko, Y. Wang, P. H. Nguyen, and C. Turkay. Supporting story synthesis: Bridging the gap between visual analytics and storytelling. *IEEE Transactions on Visualization and Computer Graphics*, pp. 1–1, 2019. doi: 10.1109/TVCG.2018.2889054
- [20] W. Chen, Z. Huang, F. Wu, M. Zhu, H. Guan, and R. Maciejewski. Vaud: A visual analysis approach for exploring spatio-temporal urban data. *IEEE Transactions on Visualization and Computer Graphics*, 24(9):2636–2648, Sep. 2018. doi: 10.1109/TVCG.2017.2758362
- [21] W. Chen, J. Xia, X. Wang, Y. Wang, J. Chen, and L. Chang. Relationlines: Visual reasoning of egocentric relations from heterogeneous urban data. *ACM Transactions on Intelligent Systems and Technology (TIST) - Special Issue on Visual Analytics*, 10(1):1–21, Dec 2018. doi: 10.1145/3200766
- [22] M. Cho, B. Kim, H. Bae, and J. Seo. Stroscope: Multi-scale visualization of irregularly measured time-series data. *IEEE Transactions on Visualization and Computer Graphics*, 20(5):808–821, May 2014. doi: 10.1109/TVCG.2013.2297933
- [23] M. Cotton, J. Wepman, J. Kub, S. Engelking, Y. Lo, H. Ottke, R. Kaiser, D. Anderson, M. Souryal, and M. Ranganathan. An overview of the NTIA/NIST spectrum monitoring pilot program. In *Proceedings of the 2015 IEEE Wireless Communications and Networking Conference Workshops (WCNCW)*, pp. 217–222. IEEE, Mar 2015. doi: 10.1109/WCNCW.2015.7122557
- [24] T. Crnovrsanin, C. Muelder, and K. Ma. A system for visual analysis of radio signal data. In *Proceedings of the 2014 IEEE Conference on Visual Analytics Science and Technology (VAST)*, pp. 33–42. IEEE, Oct 2014. doi: 10.1109/VAST.2014.7042479
- [25] R. J. Crouser, L. Franklin, A. Endert, and K. Cook. Toward theoretical techniques for measuring the use of human effort in visual analytic systems. *IEEE Transactions on Visualization and Computer Graphics*, 23(1):121–130, Jan 2017. doi: 10.1109/TVCG.2016.2598460
- [26] W. Cui, S. Liu, L. Tan, C. Shi, Y. Song, Z. Gao, H. Qu, and X. Tong. Textflow: Towards better understanding of evolving topics in text. *IEEE Transactions on Visualization and Computer Graphics*, 17(12):2412–2421, Dec 2011. doi: 10.1109/TVCG.2011.239
- [27] W. Cui, S. Liu, Z. Wu, and H. Wei. How hierarchical topics evolve in large text corpora. *IEEE Transactions on Visualization and Computer Graphics*, 20(12):2281–2290, Dec 2014. doi: 10.1109/TVCG.2014.2346433
- [28] A. D’Amico and M. Kocka. Information assurance visualizations for specific stages of situational awareness and intended uses: lessons learned. In *Proceedings of the 2005 IEEE Workshop on Visualization for Computer Security*, pp. 107–112. IEEE, Oct 2005. doi: 10.1109/VIZSEC.2005.1532072
- [29] C. Deng, J. Song, R. Sun, S. Cai, and Y. Shi. Griden: An effective grid-based and density-based spatial clustering algorithm to support parallel computing. *Pattern Recognition Letters*, 109(15):81–88, Jul 2018. doi: 10.1016/j.patrec.2017.11.011
- [30] M. Di Bartolomeo and Y. Hu. There is more to streamgraphs than movies: Better aesthetics via ordering and lassoing. *Computer Graphics Forum*, 35(3):341–350, Jul 2016. doi: 10.1111/cgf.12910
- [31] D. Edge, N. H. Riche, J. Larson, and C. White. Beyond tasks: An activity typology for visual analytics. *IEEE Transactions on Visualization and Computer Graphics*, 24(1):267–277, Jan 2018. doi: 10.1109/TVCG.2017.2745180
- [32] M. R. Endsley. Toward a theory of situation awareness in dynamic systems. *Human Factors*, 37(1):32–64, Mar 1995. doi: 10.1518/001872095779049543
- [33] M. Ester, H.-P. Kriegel, J. Sander, and X. Xu. A density-based algorithm for discovering clusters a density-based algorithm for discovering clusters in large spatial databases with noise. In *Proceedings of the Second International Conference on Knowledge Discovery and Data Mining*, pp. 226–231, Aug 1996.
- [34] Y.-a. Geng, Q. Li, R. Zheng, F. Zhuang, R. He, and N. Xiong. Recome: A new density-based clustering algorithm using relative knn kernel density. *Information Sciences*, 436:13–30, Apr 2018. doi: 10.1016/j.ins.2018.01.013
- [35] A. Gogolou, T. Tsandilas, T. Palpanas, and A. Bezerianos. Comparing similarity perception in time series visualizations. *IEEE Transactions on Visualization and Computer Graphics*, 25(1):523–533, Jan 2019. doi: 10.1109/TVCG.2018.2865077
- [36] J. R. Goodall, E. D. Ragan, C. A. Steed, J. W. Reed, G. D. Richardson, K. M. T. Huffer, R. A. Bridges, and J. A. Laska. Situ: Identifying and explaining suspicious behavior in networks. *IEEE Transactions on Visualization and Computer Graphics*, 25(1):204–214, Jan 2019. doi: 10.1109/TVCG.2018.2865029
- [37] X. Han, C. Zhang, W. Lin, M. Xu, B. Sheng, and T. Mei. Tree-based visualization and optimization for image collection. *IEEE Transactions on Cybernetics*, 46(6):1286–1300, June 2016. doi: 10.1109/TCYB.2015.2448236
- [38] M. Hao, U. Dayal, D. Keim, and T. Schreck. Multi-resolution techniques for visual exploration of large time-series data. In *Proceedings of the 9th Joint Eurographics / IEEE VGTC Symposium on Visualization*, pp. 1–8. IEEE, May 2007. doi: 10.2312/VisSym/EuroVis07/027-034
- [39] A. Hassan, C. Fluke, and D. Barnes. Interactive visualization of the largest radioastronomy cubes. *New Astronomy*, 16(2):100–109, 2011. doi: 10.1016/j.newast.2010.07.009

- [40] S. Havre, E. Hetzler, P. Whitney, and L. Nowell. Themeriver: visualizing thematic changes in large document collections. *IEEE Transactions on Visualization and Computer Graphics*, 8(1):9–20, Jan 2002. doi: 10.1109/2945.981848
- [41] R. Kincaid. Signallens: Focus+context applied to electronic time series. *IEEE Transactions on Visualization and Computer Graphics*, 16(6):900–907, Nov 2010. doi: 10.1109/TVCG.2010.193
- [42] S. Ko, J. Zhao, J. Xia, S. Afzal, X. Wang, G. Abram, N. Elmqvist, L. Kne, D. Van Riper, K. Gaither, S. Kennedy, W. Tolone, W. Ribarsky, and D. S. Ebert. Vasa: Interactive computational steering of large asynchronous simulation pipelines for societal infrastructure. *IEEE Transactions on Visualization and Computer Graphics*, 20(12):1853–1862, Dec 2014. doi: 10.1109/TVCG.2014.2346911
- [43] M. Krstajic, E. Bertini, and D. Keim. Cloudlines: Compact display of event episodes in multiple time-series. *IEEE Transactions on Visualization and Computer Graphics*, 17(12):2432–2439, Dec 2011. doi: 10.1109/TVCG.2011.179
- [44] K. Lakkaraju, W. Yurcik, and A. J. Lee. Nvisionip: Netflow visualizations of system state for security situational awareness. In *Proceedings of the 2004 ACM Workshop on Visualization and Data Mining for Computer Security*, pp. 65–72. ACM, 2004. doi: 10.1145/1029208.1029219
- [45] J. Li, S. Chen, K. Zhang, G. Andrienko, and N. Andrienko. Cope: Interactive exploration of co-occurrence patterns in spatial time series. *IEEE Transactions on Visualization and Computer Graphics*, 25(8):2554–2567, Aug 2019. doi: 10.1109/TVCG.2018.2851227
- [46] P. Liu, D. Zhou, and N. Wu. Vdbscan: Varied density based spatial clustering of applications with noise. In *Proceedings of the 2007 International Conference on Service Systems and Service Management*, pp. 1–4. IEEE, June 2007. doi: 10.1109/ICSSSM.2007.4280175
- [47] S. Liu, Y. Wu, E. Wei, M. Liu, and Y. Liu. Storyflow: Tracking the evolution of stories. *IEEE Transactions on Visualization and Computer Graphics*, 19(12):2436–2445, Dec 2013. doi: 10.1109/TVCG.2013.196
- [48] Y. Livnat, J. Agutter, , and S. Foresti. Visual correlation for situational awareness. In *Proceedings of the 2005 IEEE Symposium on Information Visualization*, pp. 95–102. IEEE, Oct 2005. doi: 10.1109/INFVIS.2005.1532134
- [49] A. Malik, R. Maciejewski, S. Towers, S. McCullough, and D. S. Ebert. Proactive spatiotemporal resource allocation and predictive visual analytics for community policing and law enforcement. *IEEE Transactions on Visualization and Computer Graphics*, 20(12):1863–1872, Dec 2014. doi: 10.1109/TVCG.2014.2346926
- [50] F. Man, R. Shi, and B. He. The data mining in wireless spectrum monitoring application. In *Proceedings of the 2017 IEEE 2nd International Conference on Big Data Analysis (ICBDA)*, pp. 223–227. IEEE, Mar 2017. doi: 10.1109/ICBDA.2017.8078812
- [51] G. E. Marai. Activity-centered domain characterization for problem-driven scientific visualization. *IEEE Transactions on Visualization and Computer Graphics*, 24(1):913–922, Jan 2018. doi: 10.1109/TVCG.2017.2744459
- [52] M. Ogawa and K.-L. Ma. Software evolution storylines. In *Proceedings of the 2010 5th International Symposium on Software Visualization*, pp. 35–42. ACM, Oct 2010. doi: 10.1145/1879211.1879219
- [53] C. Onwubiko. Functional requirements of situational awareness in computer network security. In *Proceedings of the 2009 IEEE International Conference on Intelligence and Security Informatics*, pp. 209–213. IEEE, June 2009. doi: 10.1109/ISI.2009.5137305
- [54] V. M. Patil and S. R. Patil. A survey on spectrum sensing algorithms for cognitive radio. In *Proceedings of the 2016 International Conference on Advances in Human Machine Interaction (HMI)*, pp. 1–5. IEEE, Mar 2016. doi: 10.1109/HMI.2016.7449196
- [55] A. M. M. Razip, A. Malik, S. Afzal, M. Potrawski, R. Maciejewski, Y. Jang, N. Elmqvist, and D. S. Ebert. A mobile visual analytics approach for law enforcement situation awareness. In *Proceedings of the 2014 IEEE Pacific Visualization Symposium*, pp. 169–176. IEEE, Mar 2014. doi: 10.1109/PacificVis.2014.54
- [56] A. Rodríguez and A. Laio. Clustering by fast search and find of density peaks. *Science*, 344(6191):1492–1496, June 2014. doi: 10.1126/science.1242072
- [57] B. Saket, A. Ender, and C. Demiralp. Task-based effectiveness of basic visualizations. *IEEE Transactions on Visualization and Computer Graphics*, 14(8):1–1, May 2018. doi: 10.1109/TVCG.2018.2829750
- [58] N. Sharakhov, V. Marojevic, F. Romano, N. Polys, and C. Dietrich. Visualizing real-time radio spectrum access with cornet3d. In *Proceedings of the 19th International ACM Conference on 3D Web Technologies*, pp. 109–116. ACM, 2014. doi: 10.1145/2628588.2628598
- [59] C. Shi, S. Fu, Q. Chen, and H. Qu. Vismooc: Visualizing video clickstream data from massive open online courses. In *Proceedings of the 2014 IEEE Conference on Visual Analytics Science and Technology (VAST)*, pp. 277–278. IEEE, Oct 2014. doi: 10.1109/VAST.2014.7042528
- [60] R. Shi, M. Yang, Y. Zhao, F. Zhou, W. Huang, and S. Zhang. A matrix-based visualization system for network traffic forensics. *IEEE Systems Journal*, 10(4):1350–1360, Dec 2016. doi: 10.1109/JSYST.2014.2358997
- [61] Y. Shi, C. Bryan, S. Bhamidipati, Y. Zhao, Y. Zhang, and K.-L. Ma. Meetingvis: Visual narratives to assist in recalling meeting context and content. *IEEE Transactions on Visualization and Computer Graphics*, 24(6):1918–1929, June 2018. doi: 10.1109/TVCG.2018.2816203
- [62] Y. Shi, Y. Zhao, F. Zhou, R. Shi, and Y. Zhang. A novel radial visualization of intrusion detection alerts. *IEEE Computer Graphics and Applications*, 38(6):83–95, Nov 2018. doi: 10.1109/MCG.2018.2879067
- [63] M. Steiger, J. Bernard, S. Mittelstet, H. Lcke-Tieck, D. Keim, T. May, and J. Kohlhammer. Visual analysis of time-series similarities for anomaly detection in sensor networks. *Computer Graphics Forum*, 33(3):401–410, Jul 2014. doi: 10.1111/cgf.12396
- [64] T. N. Tran, R. Wehrens, and L. M. Buydens. Knn-kernel density-based clustering for high-dimensional multivariate data. *Computational Statistics and Data Analysis*, 51(2):513–525, Nov 2006. doi: 10.1016/j.csda.2005.10.001
- [65] Z. Wang, M. Lu, X. Yuan, J. Zhang, and H. v. d. Wetering. Visual traffic jam analysis based on trajectory data. *IEEE Transactions on Visualization and Computer Graphics*, 19(12):2159–2168, Dec 2013. doi: 10.1109/TVCG.2013.228
- [66] Y. Wu, N. Cao, D. Gotz, Y. Tan, and D. A. Keim. A survey on visual analytics of social media data. *IEEE Transactions on Multimedia*, 18(11):2135–2148, Nov 2016. doi: 10.1109/TMM.2016.2614220
- [67] J. Xia, F. Ye, W. Chen, Y. Wang, W. Chen, Y. Ma, and A. K. H. Tung. Ldscanner: Exploratory analysis of low-dimensional structures in high-dimensional datasets. *IEEE Transactions on Visualization and Computer Graphics*, 24(1):236–245, Jan 2018. doi: 10.1109/TVCG.2017.2744098
- [68] C. Xie, W. Chen, X. Huang, Y. Hu, S. Barlowe, and J. Yang. Vaet: A visual analytics approach for e-transactions time-series. *IEEE Transactions on Visualization and Computer Graphics*, 20(12):1743–1752, Dec 2014. doi: 10.1109/TVCG.2014.2346913
- [69] K. Xu, S. Guo, N. Cao, D. Gotz, A. Xu, H. Qu, Z. Yao, and Y. Chen. Ecglens: Interactive visual exploration of large scale ecg data for arrhythmia detection. In *Proceedings of the 2018 CHI Conference on Human Factors in Computing Systems*, pp. 663:1–663:12. ACM, Apr 2018. doi: 10.1145/3173574.3174237
- [70] P. Xu, H. Mei, L. Ren, and W. Chen. Vidx: Visual diagnostics of assembly line performance in smart factories. *IEEE Transactions on Visualization and Computer Graphics*, 23(1):291–300, Jan 2017. doi: 10.1109/TVCG.2016.2598664
- [71] X. Xu, S. Ding, M. Du, and Y. Xue. Dpcg: an efficient density peaks clustering algorithm based on grid. *International Journal of Machine Learning and Cybernetics*, 9(5):743–754, 2016. doi: 10.1007/s13042-016-0603-2
- [72] X. Yin, W. Yurcik, M. Treaster, Y. Li, and K. Lakkaraju. Visflowconnect: Netflow visualizations of link relationships for security situational awareness. In *Proceedings of the 2004 ACM Workshop on Visualization and Data Mining for Computer Security*, pp. 26–34. ACM, 2004. doi: 10.1145/1029208.1029214
- [73] Y. Zhao, F. Luo, M. Chen, Y. Wang, J. Xia, F. Zhou, Y. Wang, Y. Chen, and W. Chen. Evaluating multi-dimensional visualizations for understanding fuzzy clusters. *IEEE Transactions on Visualization and Computer Graphics*, 25(1):12–21, Jan 2018. doi: 10.1109/TVCG.2018.2865020
- [74] F. Zhou, X. Lin, C. Liu, Y. Zhao, P. Xu, L. Ren, T. Xue, and L. Ren. A survey of visualization for smart manufacturing. *Journal of Visualization*, 22(2):419–435, 2019. doi: 10.1007/s12650-018-0530-2
- [75] F. Zhou, X. Lin, X. Luo, Y. Zhao, Y. Chen, N. Chen, and W. Gui. Visually enhanced situation awareness for complex manufacturing facility monitoring in smart factories. *Journal of Visual Languages and Computing*, 44:58–69, 2018. doi: 10.1016/j.jvlc.2017.11.004
- [76] Z. Zhou, L. Meng, C. Tang, Y. Zhao, Z. Guo, M. Hu, and W. Chen. Visual abstraction of large scale geospatial origin-destination movement data. *IEEE Transactions on Visualization and Computer Graphics*, 25(1):43–53, Jan 2019. doi: 10.1109/TVCG.2018.2864503